CDF/ANAL/EWK/CDFR/8095
March 8, 2006
Version 1.1

Measurement of the WZ Cross Section in Trileptons + Missing Transverse Energy

Shih-Chieh Hsu, Elliot Lipeles, Kevin McCarthy, Mark Neubauer, Frank Würthwein

University of California, San Diego

Abstract

In this note, we present a search for WZ production in the trileptons + $\not\!\!E_T$ channel using 824.5 pb^{-1} of integrated luminosity. Production of WZ bosons has not been conclusively observed and is unavailable at e^+e^- experiments. Aside from being an important background for new physics searches in trileptons, WZ production provides a model-independent test of the WWZ trilinear electroweak gauge coupling. We expect 3.72 ± 0.02(stat.) ± 0.15(syst.) events of signal and $0.91 \pm 0.07(stat.)^{+0.16}_{-0.10}(syst.)$ events of background. We observe two trilepton candidates passing our selection, consistent both with a fluctuation of the background alone as well as the background + signal expectation. Using these results, we set a limit on the WZ cross section at $\sqrt{s} = 1.96$ TeV of 6.35 pb at 95% confidence.

Contents

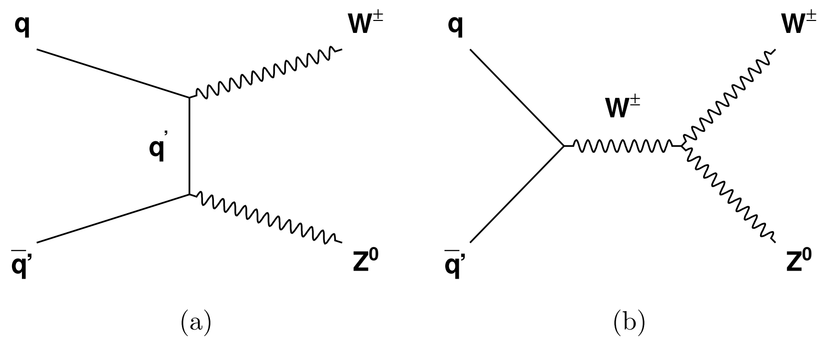

Figure 1: Leading-order diagrams contributing WZ production at the Tevatron

1 Introduction

In $p\overline{p}$ collisions at the Tevatron, single W and Z bosons are copiously produced and extensively studied with the CDF detector. Diboson production (WW, WZ, ZZ), while much more rare, can produce a wealth of information on electroweak physics and provides a probe of non-Standard Model physics at the high energy frontier.

WZ production has yet to be conclusively observed and is not available in e^+e^- collisions. At the Tevatron, WZ bosons are produced via the diagrams shown in Figure 1. Measurement of WZ production can be used to make a model-independent test of the WWZ Standard Model gauge coupling via the diagram shown in Figure 1(b).

The NLO Standard Model WZ cross section is calculated using the MCFM [3] program using the CTEQ6[4] parton distribution functions to be $\sigma(p\overline{p} \to WZ) = 3.65 \pm 0.26$ pb. CDF published[2] a search for the sum of WZ and ZZ production for which the 95% C.L. upper limit of $\sigma(WZ + ZZ) < 15.2$ pb was obtained. D0 recently published a search specifically for WZ production in which they quote both a 95% C.L. upper limit of $\sigma(WZ) < 13.3$ pb and measurement of the cross section of $\sigma(WZ) = 4.5^{+3.8}_{-2.6}$ pb. The D0 search was in the trilepton + $\not{E}_T$ channel using $\sim$ 300pb^{-1} in which they observed 3 candidates (one eee and two eeμ) with an expected background of 0.71±0.08 events and expected WZ signal of 2.04±0.13 events. They state that the probability for the background alone to fluctuate to 3 or more observed events is 3.5%.

The analysis we report in the note is very much like the D0 analysis in that we specifically search for WZ production in the trileptons + $\not{E}_T$ channel. This has advantage of being a comparatively clean channel to search for WZ production at the expense of small branching fraction. The branching fraction of WZ to 3 e,μ leptons (folding in the leptonic τ branching fractions) is 1.80% which means we expect 65.7 trilepton events per fb^{-1}.

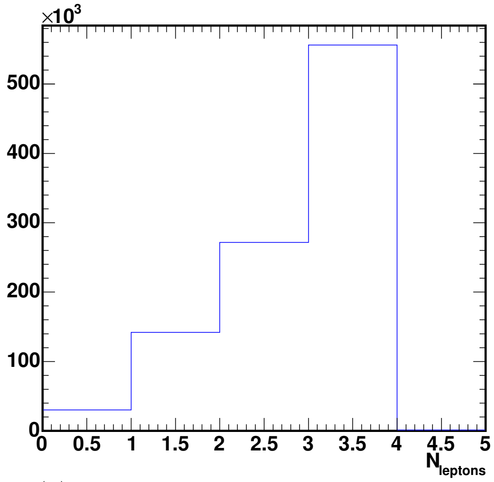

(a) Number of generated e,μ leptons

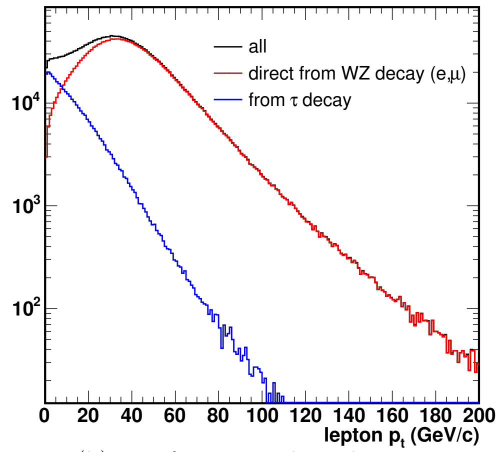

(b) $\mathrm{p_t}$ of generated e,μ leptons

Figure 2: WZ decays in generated using PYTHIA

2 Event Selection

In this section, we describe our candidate selection. This includes the trigger datasets we use in our analysis, reconstruction of low-level objects used in the selection, and our high-level cuts.

2.1 Strategy

Our strategy is to search for WZ candidates which decay to three final state leptons with missing large transverse energy ($\not\!\!E_T$). The signal $\not\!\!E_T$ is primarily from the neutrino energy in $\mathrm{W} \rightarrow \mathrm{e}\nu$ and $\mathrm{W} \rightarrow \mu\nu$ decay with possibly additional contributions from leptonic τ decays. We require one lepton to be consistent with having generated one of the high $\mathrm{p_t}$ inclusive lepton triggers and allow for the other two leptons to be identified but loosely selected and have momentum below the these trigger thresholds.

We require that there be at least two opposite charge, same flavor leptons with invariant mass near the Z mass, consistent with having originating from Z decay. In this selection, the main backgrounds are dominated by Z+X, with $\mathrm{X} \equiv \mathrm{Z}, \gamma$, or jet(s) reconstructed as an identified lepton (Z+jet "fake").

2.2 Datasets

We use the high $\mathrm{p_t}$ inclusive lepton triggers for our analysis since the majority of e or μ leptons from WZ decay are above 18 GeV in $\mathrm{p_t}$ as shown in Figure 2(b).

Specifically, we use the following three trigger paths:

- ELECTRON_CENTRAL_18
- MUON_CMUP_18
- MUON_CMX_18

The corresponding datasets for Gen5/6 data are bhel0d/0h (electrons) and bhmu0d/0h (muons). We only include runs in the following v10 good run lists:

Good run list	$\mathcal{L}$ (pb^{-1})
EM_NOSI	824.5
EM_CMUP_NOSI	803.3
EM_MU_NOSI_CMXIGNORED	747.6
EM_SI	753.9
EM_CMUP_SI	735.1
EM_MU_SI_CMXIGNORED	682.8

Table 1: Luminosity for each of the good run lists used in this analysis. These have been scaled by the factor of 1.019.

- EM_NOSI
- EM_CMUP_NOSI
- EM_MU_NOSI_CMXIGNORED
- EM_SI
- EM_CMUP_SI
- EM_MU_SI_CMXIGNORED

The luminosity of each good run list is shown in Table 2.2.

2.3 Low-level Objects

Selection begins with construction of categories of identified leptons, reconstruction of jets and calculation of the $\not\!\!E_T$ in each event. These are described in this section.

2.3.1 Lepton Identification and Categories

We use three categories of electrons and three categories of muons for this analysis. The electrons are TCE, PHX, and LCE, where LCE is a significantly loosened version of the TCE cuts. The muons are CMUP, CMX, and CMIO where CMIO is defined as a track object that passes the CMIO cuts, but does not pass the CMUP and CMX cuts. The electron and muon selection criteria are detailed in Tables 2-4.

These categories all extend down to 10 GeV E_T, but we require at least one $E_T > 20$ GeV lepton for triggering. This choice and the use of standard TCE, CMUP, and CMX selections means that the trigger efficiencies measured in notes 7939[7] and 7956[8] and shown in Table 5 for electrons and muons, respectively, are applicable.

	TCE
Region	Central
Fiducial	FidEleSmx ==1
E_T	>= 20, >= 10 (TCEL)
Track p_T	>= 10, >= 5 (TCEL)
Track $\|z_0\|$	<= 60 cm
#Ax SL (5hits)	>= 3
#St SL (5hits)	>= 2
Conversion	$! = 1$
Had/Em	$<= 0.055 + 0.00045E$
Iso/E_T	<= 0.1
Lshr	<= 0.2
E/P	$< 2.5 + 0.015 * E_T$
Signed CES ΔX	$-3 <= q\Delta X <= 1.5$ cm
$CES\|\Delta Z\|$	< 3 cm
Tracks	BcTrk (Larry's Correction if Data)

Table 2: Selection for central leptons. TCE candidates are the full table and LCE is same as TCE with the cuts in red (in the second box) removed. TCEL is the verion of the selection with an $E_T > 10$ GeV cut instead of the $E_T > 20$ GeV.

	PHX
Region	Plug
Et	10
Pes2DEta	$1.2 < \|\eta\| < 2$
Had/Em	<= 0.05
PEM3x3FitTower	true
$PEM3x3\chi^2$	<= 10
Pes5x9U	>= 0.65
Pes5x9V	>= 0.65
Iso/Et	<= 0.1
ΔR(Pes,PEM)	<= 3.0
PhxMatch	True
NSiHits	>= 3
$\|TrackZ0\|$	$<= 60cm$

Table 3: Selection for phoenix electrons

	Muon
Track p_T	$>= 10$
CMU Fid	x-fid< 0 cm z-fid< 0cm
CMP Fid	x-fid< 0 cm z-fid<-3cm
CMX Fid	x-fid< 0 cm z-fid<-3cm
E_{em}	$<= 2 + max(0, (p - 100) * 0.0115)$
E_{had}	$<= 6 + max(0, (p - 100) * 0.028)$
Iso/Pt	$<= 0.1$
NAxL(5 hits)	$>= 3$
NStL(5 hits)	$>= 2$(3 if CMIO)
Track $\|Z_0\|$	$<= 60cm$
Track $\|D_0\|$	$<= 0.2cm$ (0.02cm if NSiHit> 0)
χ^2/dof	<= 4 (3 if run <= 186598 or CMIO)
$\|\Delta X_{CMU}\|$	$<= 7cm$
$\|\Delta X_{CMP}\|$	$<= 5cm$
$\|\Delta X_{CMX}\|$	$<= 6cm$
ρ_{exit}	> 140 cm if CMX
$E_{em} + E_{had}$	$> 0.1GeV$ if CMIO
CMP veto	No Bluebeam in CMP for run < 154449
CMX veto	No CMX for run < 150144, No Miniskirt, No Keystone
Arches	Arches only for all run range
	Arches removing wedge 14 on West Side for run > 190697
Tracks	BcTrk (Larry's Correction if Data)

Table 4: Selection for CMUP, CMX, and CMIO muons

	Gen5	Gen6	CDF Note
TCE	0.9620 ± 0.006	0.9766 ± 0.006	7939
CMUP	0.8977 ± 0.005	0.9186 ± 0.004	7956
CMX	0.9665 ± 0.004	0.9586 ± 0.004	7956

Table 5: Trigger effieciencies used.

2.3.2 Jets

Jets are only used as part of the $\not\!\!E_T$ correction applied below. The jets used in this correction are selected with a cone size of ΔR <0.4 based on the JetClu algorithm. The latest level 5 corrections[1] are used to correct the absolute energy scale of the jets, but the higher level out of cone and underlying event corrections are not applied in order to avoid double counting or under counting of the energy. For purposes of jet counting, we do not count jets within $\Delta R < 0.4$ of our reconstructed leptons.

2.3.3 Missing Transverse Energy ($\not\!\!E_T$)

The $\not\!\!E_T$ calculation used for this analysis starts with the sum of the transverse energy over the entire calorimeter using the highest $\sum p_T$ vertex to define the directions. The $\not\!\!E_T$ is then corrected for the identified muons by subtracting the muons p_T and adding back its calorimeter E_T. Finally the $\not\!\!E_T$ is corrected for jets $E_T > 15$ GeV and $|\eta| < 2.5$ which do not $\Delta R < 0.4$ match any identified leptons in the event, by subtracting the corrected jet E_T and adding back the raw E_T. Detailed studies validating and quantifying the $\not\!\!E_T$ calculation and simulation are described in our note[11] documenting the $WW \rightarrow l\nu l\nu$ analysis.

2.4 High-level Cuts

This section describes the high-level cuts we make in our trilepton selection. We require there to be 3 and only 3 reconstructed leptons passing our lepton identification cuts. We do not make any selection on the number of jets in the event, as $t\bar{t}$ background is expected to be small in the trilepton mode.

2.4.1 Cosmic Rays

To reject cosmic ray events contaminating our muon candidates, we veto events tagged as di-cosmic by the CosmicFinderModule. This is equivalent to requiring the HasNotOutgoingPair $! = 1$ from the TStnCosmicBlock in Stntuple.

2.4.2 Δz_0

Since the WZ events we are searching for have decay daughters that originate from a common vertex, we require that the z_0 of the three reconstructed tracks be sufficiently close. This will reduce contamination from poorly reconstructed tracks, cosmics, multiple interactions, etc. Our selection requires that the maximum Δz_0 between pairs of our trilepton candidate be less than 4 cm. This cut accepts >99.5% of the WZ signal based upon our reconstructed PYTHIA WZ sample.

[1]based upon the jetCorr05b tag of JetUser package

2.4.3 Z Mass Region

Since we are searching for WZ reconstructed in the trilepton mode, we require there be at least two opposite charge, same flavor leptons with invariant mass near the Z mass, consistent with having originating from Z decay. Since we expect the dominant backgrounds to involve a decay of Z boson, we are actually not very sensitive to the choice of Z mass window in the trilepton mode. We chose to choose a Z mass window of ($76 < \mathrm{M_{l+l-}} < 106$ GeV) which the same used in the previous WZ(+ZZ) analysis[6].

2.4.4 ZZ Veto

The decay of ZZ where both Z bosons decay to charged leptons can enter our trilepton selection when one of the leptons does not pass our identification cuts. A HEPG study of ZZ decays reconstructed in the trilepton mode shows that the are three main cases (i) decays involving τ's where one τ decays leptonically and the other hadronically (ii) lepton falls into region where do not have ID acceptance but do have tracking acceptance (e.g. crack), and (iii) same as (ii) but do not have a track (e.g. forward muons). For (ii), we can recover these as ZZ background by looking for one or more isolated tracks (track isolation in $\Delta R = 0.4$ cone of less than 0.1) which make a Z mass ($76 < \mathrm{M_{l+l-}} < 106$ GeV) with the lepton not involved in making the Z region cut previously mentioned. We find this cut reduces the ZZ background by ∼40% with negligible effect on the WZ signal. Figure 3 shows the invariant mass of this second lepton/track pair versus $\Delta\phi(\not\!\!E_T, trk)$, showing that the majority of the time the $\not\!\!E_T$ points along the direction of the non-ID'd track.

2.4.5 $\not\!\!E_T$

$\not\!\!E_T$ is the most powerful high-level cut for removing backgrounds from the WZ search region. We require $\not\!\!E_T > 25$ GeV in our event selection. Figure 4(a) shows the reconstructed $\not\!\!E_T$ for WZ signal and physics backgrounds, scaled to the expected number of events in our dataset. The selection of our $\not\!\!E_T$ cut is based upon Figure 4(b) for the reconstructed $\not\!\!E_T$ of WZ and ZZ MC after all other selection cuts.

3 Signal and Background Expectations

In this section, we present the acceptance for our WZ signal and the expected yields for signal and the backgrounds we consider.

3.1 Monte Carlo Samples

The geometric and kinematic acceptance for signal and backgrounds (except fakes) are determined from Monte Carlo using a full GEANT-based simulation of the detector. Table 6 lists all the samples used. Here we give brief notes on the samples.

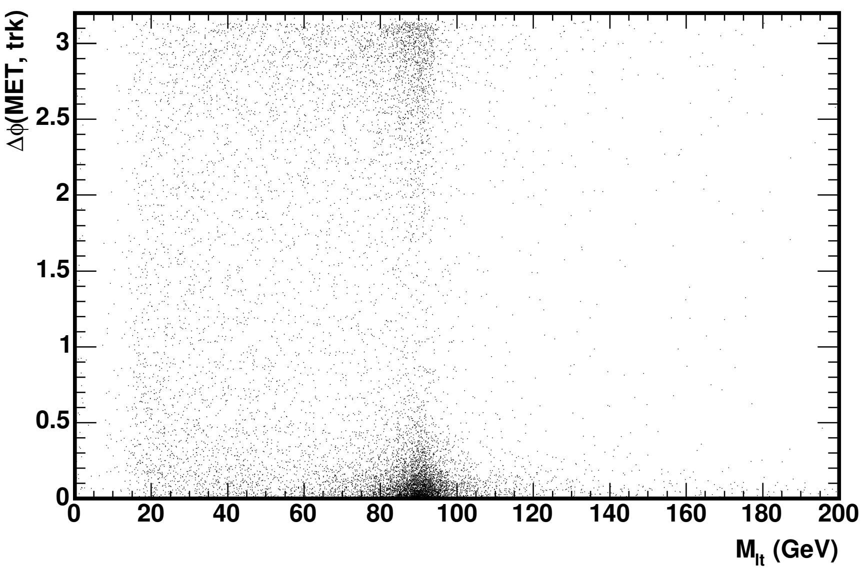

Figure 3: Invariant mass of this second lepton/track pair versus $\Delta\phi(\not{E}_T, trk)$ for the Pythia ZZ sample.

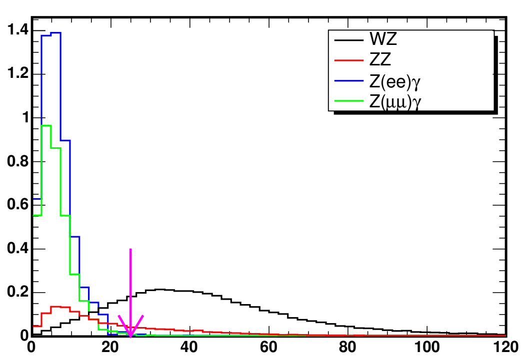

(a) Reconstructed $\not{E}_T$ for WZ signal and backgrounds, scaled to the expected number of events in our dataset

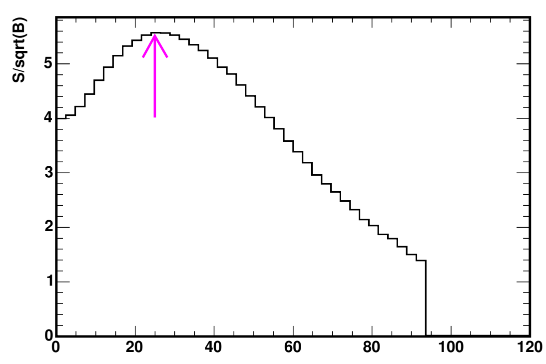

(b) Optimization for $\not{E}_T$ cut, considering only WZ and ZZ

3.1.1 Heavy dibosons: WW, WZ, ZZ

The WZ and ZZ samples we use are based upon the PYTHIA event generator. The WZ samples are decayed with the Z decaying to a pair of e, μ, or τ leptons, and the W decaying generically, which is then filtered for two e or μ leptons above 1 GeV. The ZZ sample is constructed with both Z's decaying generically and then then filtered for two e or μ leptons above 1 GeV. The ZZ Monte Carlo includes γ^* component (and simulates the interference) and has an $\mathrm{M_Z} > 15$ GeV generator-level requirement.

3.1.2 $Z\gamma$

The $Z\gamma$ Monte Carlo used for this analysis uses the Baur matrix element generator [5] which is passed to PYTHIA via the LesHouchesModule. Because of some indecision over the proper settings for the PYTHIA QED radiation settings the Gen5 sample has the QED turned off and the Gen6 sample has it turned on. In both the $Z\gamma \to ee\gamma$ and $Z\gamma \to \mu\mu\gamma$ samples, the QED radiation setting in PYTHIA was turned off. Effects from QED radiation are small for this analysis compared to uncertainties from the conversion finding efficiency and K-factor uncertainties.

3.1.3 $t\bar{t}$

The $t\bar{t}$ sample is generated at a mass of 175 GeV, uses Gen5 for the full run range and has no minbias in the events. The NLO cross section is 6.7±0.7 pb.

3.1.4 $Z \to ee$ and $Z \to \mu\mu$

The $Z \to ee$ and $Z \to \mu\mu$ samples are generated with a 20 GeV minimum dilepton mass. They uses Gen5 for the 0d run range and Gen6 for the 0h run range. They have a full luminosity dependent addition of minbias in the events.

3.2 Acceptance calculation

Determinaton of the acceptance is made separately for each of our trilepton categories. Each category is corrected for the lepton identification scale factors and trigger efficiencies that are relevant to that specific trilepton category and for the relative luminosity of applicable good run list to the EM_NOSI good run list. The master formula is then

$$A_i = \frac{N_{\mathrm{reco}}}{N_{\mathrm{gen}}(|Z_0| < 60 \text{ cm})} \times \epsilon_{trg} \times s_{lep} \times \epsilon_{vtx} \times \frac{\mathcal{L}_i}{\mathcal{L}_{\mathrm{em\_nosi}}} \quad (1)$$

where $A\epsilon$ is the acceptance times the efficiency and

- N_{reco} is the number of reconstructed events passing the full selection,

mode	Gen	Dataset	$\sigma \times \mathcal{B}()$	K-factor[a]	Filter Eff
$t\bar{t}$	5	ttopkl/yl	6.7	1.0	1.0
$t\bar{t}$	6	ttoptl/vl	6.7	1.0	1.0
WZ	5	wewk6d	0.365	1.0	0.76
WZ	6	wewk6d	0.365	1.0	0.76
ZZ	5	wewk7d	2.01	1.0	0.23
ZZ	6	wewk7d	2.01	1.0	0.23
$Z \to ee$	5	sewkdd	355.2	1.4	1.0
$Z \to ee$	6	zewk6d	355.3	1.4	1.0
$Z \to \mu\mu$	5	zewk6m	355.3	1.4	1.0
$Z \to \mu\mu$	6	zewk6m	355.3	1.4	1
$Z\gamma \to ee\gamma$	5	rewk03	10.34	1.3	1
$Z\gamma \to \mu\mu\gamma$	5	rewk04	10.34	1.3	1

[a] If cross-section is NLO then K-factor is one.

Table 6: Monte Carlo samples used in this analysis

- $N_{\rm gen}(|Z_0| < 60$ cm) is the number of generated events with 60 cm of the interaction point
- ϵ_{trg} is the effective trigger efficiency for the category (see below),
- s_{lep} is the effective lepton id scale factor (see below),
- ϵ_{vtx} is $0.9555 \pm 0.0004(stat) \pm 0.0031(sys)$ from CDF note 7935, and
- $\frac{\mathcal{L}_i}{\mathcal{L}_{\rm em\_nosi}}$ accounts for the relative amount of the applicable good run list.

The detailed definition of $\frac{N_{\rm reco}}{N_{\rm gen}(|Z_0|<60 \text{ cm})}$ actually slightly different for WZ signal and background. For signal, this is the fraction of generated trilepton events (e or μ direct from the WZ or from subsequent leptonic tau decay) that pass our reconstruction. For the backgrounds, this is the fraction of generated events in the sample that are reconstructed as trileptons and pass our full selection, which each reconstructed lepton matched at the HEPG level to generated e or μ lepton (or $\gamma > 5$ GeV, relevant for $Z\gamma$).

3.2.1 Lepton Id Scale Factors

The lepton id scale factors and uncertainties for electrons and muons are summarized in Table 8. They are discussed in detail in CDF Note 8093 [10], including the measurement procedure for the low pt scale factors (see Table 8). These are applied by simply multiplying together the scale factor for each lepton type assuming that they are completely uncorrelated.

Type	Gen5	Gen6
TCE	0.928 ± 0.022	0.963 ± 0.019
LooseCEM	0.984 ± 0.014	1.016 ± 0.011
PHX	0.998 ± 0.079	0.930 ± 0.048
CMUP	0.935 ± 0.039	0.896 ± 0.041
CMIO	1.003 ± 0.026	1.026 ± 0.020
CMX	0.975 ± 0.043	1.060 ± 0.028

Table 7: Electron and muon ID scale factor measurements for $10 > E_T > 20$ GeV. Details of the procedure are described in [10].

Type	Gen5	Gen6
TCE	0.9943 ± 0.0031 (0.0700)	0.9885 ± 0.0030 (0.0322)
LooseCEM	0.9897 ± 0.0022 (0.0155)	0.9890 ± 0.0021 (0.0293)
PHX	0.9322 ± 0.0061 (0.1027)	0.9155 ± 0.0056 (0.0502)
CMUP	0.9314 ± 0.0057 (0.039)	0.9296 ± 0.0060 (0.053)
CMIO	1.0050 ± 0.0051 (0.026)	1.0136 ± 0.0049 (0.024)
CMX	0.9981 ± 0.0060 (0.049)	0.9894 ± 0.0068 (0.076)

Table 8: Electron and muon ID scale factors. The uncertainty shown is the value used for $E_T > 20$ GeV. In parentheses is the uncertainty used for $10 > E_T > 20$ GeV. This is a combination of the difference between the low pt and high pt averaged scale factors and the statistical uncertainty on the low pt scale factor determination.

category	base	Z Mass	ZZ Veto	$\not\!\!E_T > 25$ GeV
WZ				
e e e	$(2.81 \pm 0.02)\%$	$(2.50 \pm 0.02)\%$	$(2.48 \pm 0.02)\%$	$(1.99 \pm 0.02)\%$
e e μ	$(2.45 \pm 0.02)\%$	$(2.07 \pm 0.02)\%$	$(2.05 \pm 0.02)\%$	$(1.63 \pm 0.01)\%$
e μ μ	$(2.35 \pm 0.02)\%$	$(2.09 \pm 0.02)\%$	$(2.08 \pm 0.02)\%$	$(1.66 \pm 0.01)\%$
μ μ μ	$(2.12 \pm 0.02)\%$	$(1.98 \pm 0.02)\%$	$(1.98 \pm 0.02)\%$	$(1.58 \pm 0.01)\%$
Total	$(9.73 \pm 0.03)\%$	$(8.59 \pm 0.03)\%$	$(8.59 \pm 0.03)\%$	$(6.87 \pm 0.03)\%$

Table 9: WZ signal acceptance as defined in the text. The "base" column includes lepton ID, good run, trigger lepton, cosmic rejection, and Δz_0 requirements.

3.2.2 Trigger Efficiencies

The trigger efficiencies are applied using the expression:

$$\epsilon_{trg} \quad = \quad 1 - (1 - \epsilon_{trg}^{\text{leg 1}}) \times (1 - \epsilon_{trg}^{\text{leg 2}}) \times (1 - \epsilon_{trg}^{\text{leg 3}}) \tag{2}$$

where $\epsilon_{trg}^{\text{leg 1,2,3}}$ are the trigger efficiencies for each leg. If one leg is not triggerable then its efficiency is set to zero. In order to count as a triggerable leg, the leg must satisfy the TCE, CMUP, or CMX lepton criteria with $\mathrm{E_t} > 20$ GeV and match to a L3 trigger object.

3.3 Signal

Table 9 shows the fraction of generated WZ$\rightarrow$ 3 e, μ leptons (including e, μ leptons from τ's) that pass our selection cuts. Table 10 shows the expected WZ signal yield for the full dataset after selection cuts. This signal yield is in good agreement with the expectation from [6] of 3.7 events when one scales up their WZ trilepton channel from 0.78 events by $\times 4$ for luminosity and $\sim 20\%$ one expects from the gain in acceptance for allowing the subleading legs to be > 10 GeV from > 20 GeV.

3.4 Backgrounds

We estimate the backgrounds to our WZ signal using a combination of Monte Carlo and data. The background acceptance for ZZ, Zγ and $t\bar{t}$ are determined from the Monte Carlo samples and scaled by the appropriate factors for cross section $\times$ branching fraction, filter efficiency, and luminosity to arrive at expected yields corresponding to our dataset and selection. The background due to jet fakes are determined from data.

category	base	Z Mass	ZZ Veto	$\not\!\!E_T > 25$ GeV
WZ				
e e e	1.525 ± 0.010	1.355 ± 0.009	1.343 ± 0.009	1.079 ± 0.008
e e μ	1.325 ± 0.009	1.121 ± 0.008	1.112 ± 0.008	0.885 ± 0.007
e μ μ	1.275 ± 0.009	1.132 ± 0.008	1.126 ± 0.008	0.901 ± 0.008
μ μ μ	1.147 ± 0.008	1.076 ± 0.008	1.071 ± 0.008	0.858 ± 0.007
Total	5.272 ± 0.018	4.683 ± 0.017	4.652 ± 0.017	3.724 ± 0.015

Table 10: Expected signal and background yields in the full data set over our good run list. The "base" column includes lepton ID, good run, trigger lepton, cosmic rejection, and Δz_0 requirements.

3.4.1 ZZ

The ZZ process contributes to our trilepton sample when each Z decays leptonically and either one of the e,μ leptons is not identified or a generated τ from a Z decays hadronically. Recall that the former situation is mitigated by searching for an isolated track in addition to our reconstructed trileptons which makes a Z mass with the lepton remaining after the opposite-sign same-flavor Z selection.

We use the wewk7d PYTHIA MC sample to generate our ZZ acceptance and event yield expectations. In the case of ZZ, PYTHIA includes the γ^* component for each Z and simulates the interference between the two. Therefore, a simple counting of the fraction of reconstructed trileptons from generated events underestimates the background. To account for the γ^* component in the cross-section, we have run the MCFM to calculate the NLO cross section with the $\gamma*$ component and M(Z)>15 GeV to be 2.01 pb.

The total background from ZZ is estimated to be 0.498 ± 0.007 events.

3.4.2 Zγ

The Zγ mode enters our selection when the photon is reconstructed as an electron and we also have large $\not\!\!E_T$. This is usually due to a conversion. In the TCE selection, we explicitly veto conversions, but the efficiency of this veto may not be well modeled in the Monte Carlo. In CDF Note 8073[9] Attal et al. measure a conversion veto scale factor by identifying conversions using the CES and then determining the rate at which they are vetoed. For the energy range $E_T > 10$ GeV, they find an scale factor of $\approx 1.3 \pm 0.1$. In the plug region, the conversion rate is sensitive to the material description in the Monte Carlo which is not tuned perfectly.

Based on the conversion veto scale factor, we scale the $Z\gamma$ up by 1.3. The total background from Zγ is estimated to be 0.03 ± 0.01 events from the sum of $Z\gamma \rightarrow \mu\mu\gamma$ and $Z\gamma \rightarrow ee\gamma$ contributions.

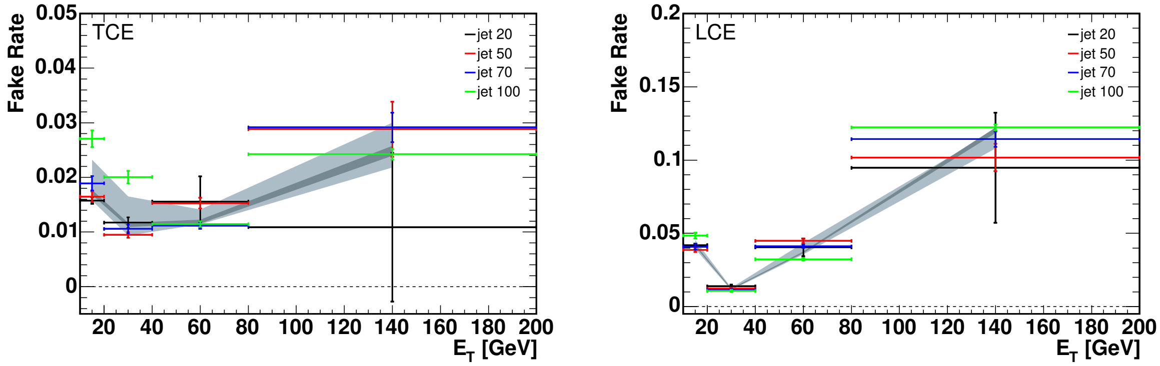

(c) TCE Fake Rate

(d) LCE Fake Rate

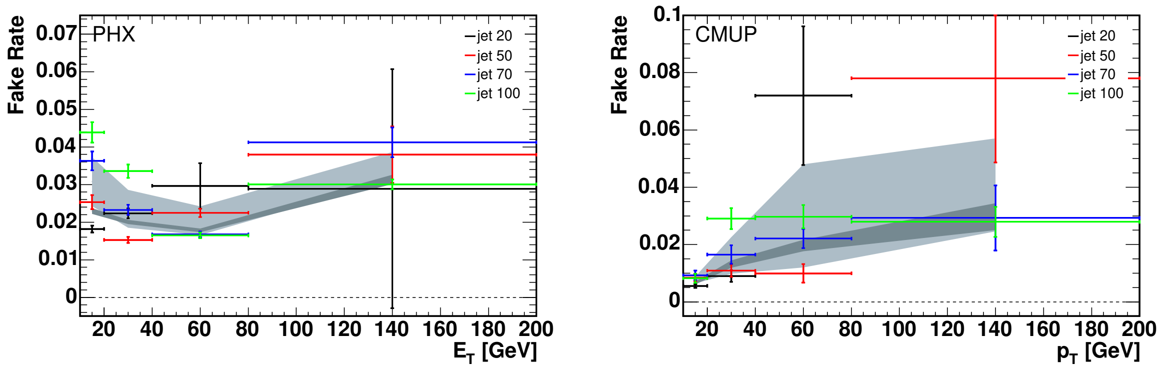

(e) PHX Fake Rate

(f) CMUP Fake Rate

Figure 4: Fake rates, f_i, measured in the jet samples averaged over Gen5 and Gen6.

3.4.3 $t\bar{t}$

In the trilepton channel, $t\bar{t}$ is expected be a small background so we do not make a jet multiplicity requirement ($t\bar{t}$ contributes mainly to $N_{jets} \geq 2$.) The total background from $t\bar{t}$ is estimated to be 0.047 ± 0.010 events.

3.4.4 Fakes from Z+jets

The WZ$\rightarrow$ trilepton signal has a background from the Z+jet(s) process when one of the jets is reconstructed as identified lepton. The lepton fake probabilities ("rates") are measured in the inclusive jet samples after corrections are made for small contributions from real isolated leptons from electroweak processes. The details of this determination and application of the fake rates to obtain fake background yields are described in detail in CDF Note 8093[10], so we only summarize them here.

The fakes rate for each type of lepton is shown in Figure 4 and 5. These represent the probability of a loosely selected "lepton" (sufficiently looser than the full ID, referred to as "denominator objects" or "fakeable objects") in a jet to be identified as real lepton in our reconstruction. Tables 11-13 detail the denominators definition we use in our analysis.

We apply the fake rates to the data in the following manner. Events are selected from our data using the same trilepton selection criteria except that the third lepton is selected as a denominator object rather than an identified lepton. We then apply the fake rate to the denominators in this "dilepton + denominator object" dataset to arrive at the expected number of trilepton background events from Z+jet(s). In this case, one of the

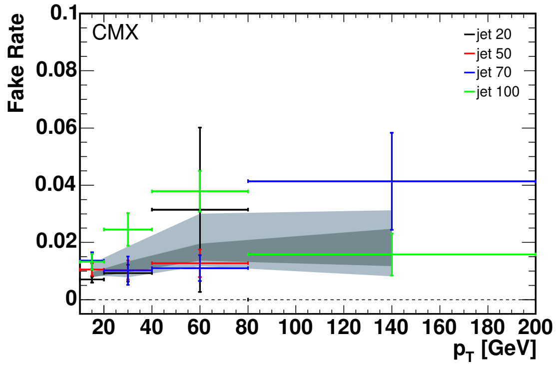

(a) CMX Fake Rate

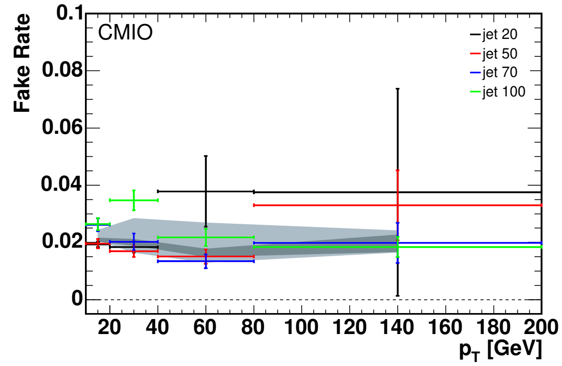

(b) CMIO Fake Rate

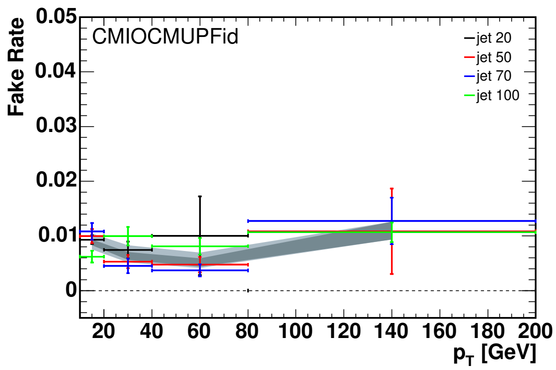

(c) CMIO-CMUPFiducial Fake Rate

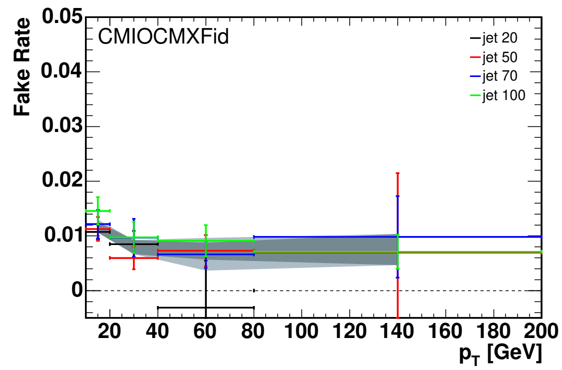

(d) CMIO-CMXFiducial Fake Rate

Figure 5: Fake rates, f_i, measured in the jet samples averaged over Gen5 and Gen6.

	FakeCEMObject
Detector	CEM
Et	$>= 10$
Conversion	$! = 1$
Had/Em	$<= 0.125$
Iso/Et	$<= 0.2$
Tracks	defTrack (BcTrk if no SiHits)

Table 11: Fakeable CEM denominator definition

	FakePEMObject
Detector	PEM
Et	$>= 10$
Pes2DEta	$1.2 < \|\eta\| < 2$
Had/Em	$<= 0.125$
Iso/Et	$<= 0.2$
PhxMatch	true

Table 12: Fakeable PEM denominator definition

	FakeMuonObject
TrackPt	>= 10
CMU Fid	x-fid< 0 cm z-fid< 0cm
CMP Fid	x-fid< 0 cm z-fid<-3cm
CMX Fid	x-fid< 0 cm z-fid<-3cm
(Eem+Ehad)/P	<= 1
Iso/Pt	<= 0.1
NAXL(5hits)	>= 2
NSTL(5hits)	>= 2
$\lvert TrackZ0 \rvert$	<= 60 cm
$TrackD0$	<= 0.2 cm (0.02cm if NSiHit> 0)
CMP veto	No BlueBeam in CMP for run < 154449
CMX veto	No CMX for run < 150144
	Arches only for all run range
	Arches removing wedge 14 on West Side for run > 190697
Tracks	defTrack (BcTrk if no SiHits)

Table 13: Fakeable Muon denominator definition

dileptons is required to pass the trigger criteria.

An additional contribution to the fake background is added for events in which the dilepton candidates are not triggerable, but the denominator object is triggerable. This contribution is estimated using Drell-Yan Monte Carlo to determine the fraction of such events and then this fraction is multiplied by the triggerable dilepton+fake expectation to arrive at the expected background yield.

The total background from fakes using this procedure is estimated to be 0.34 ± 0.07 events.

3.4.5 Summary

Table 14 summarizes the expected background yields for the full dataset after selection cuts for ZZ, Zγ, and $t\bar{t}$ physics processes. Table 15 shows the fake background contribution. We expect a total of 0.91$\pm$0.07 background events with a WZ signal expectation of 3.72$\pm$0.02, where errors are statistical only.

4 Cross checks

The trilepton channel for the WZ process has one relevant control region; namely trileptons reconstructed in the Z mass but low $\not\!\!E_T$. In this region, we expect background from

category	base	Z Mass	ZZ Veto	$\not\!\!E_T > 25$ GeV
ZZ				
e e e	0.692 ± 0.009	0.585 ± 0.008	0.456 ± 0.007	0.090 ± 0.003
e e μ	0.626 ± 0.008	0.498 ± 0.007	0.325 ± 0.006	0.171 ± 0.004
e μ μ	0.630 ± 0.008	0.520 ± 0.008	0.402 ± 0.007	0.072 ± 0.003
μ μ μ	0.566 ± 0.008	0.495 ± 0.007	0.323 ± 0.006	0.165 ± 0.004
Total	2.514 ± 0.017	2.097 ± 0.015	1.505 ± 0.013	0.498 ± 0.007
$Z(e^+e^-)\gamma$				
e e e	14.194 ± 0.267	5.267 ± 0.163	5.251 ± 0.163	0.017 ± 0.009
$Z(\mu^+\mu^-)\gamma$				
e μ μ	9.839 ± 0.225	3.511 ± 0.134	3.504 ± 0.134	0.008 ± 0.006
$t\bar{t}$				
e e e	0.060 ± 0.011	0.027 ± 0.007	0.027 ± 0.007	0.025 ± 0.007
e e μ	0.102 ± 0.015	0.015 ± 0.006	0.015 ± 0.006	0.015 ± 0.006
e μ μ	0.050 ± 0.010	0.008 ± 0.004	0.008 ± 0.004	0.006 ± 0.004
Total	0.212 ± 0.021	0.050 ± 0.010	0.050 ± 0.010	0.047 ± 0.010
Sum of backgrounds				
e e e				0.132 ± 0.012
e e μ				0.186 ± 0.007
e μ μ				0.086 ± 0.007
μ μ μ				0.165 ± 0.004
Total				**0.569 ± 0.016**

Table 14: Expected background yields (without fakes) in the full data set over our good run list. The "base" column includes lepton ID, good run, trigger lepton, cosmic rejection, and Δz_0 requirements.

category	Triggerable Dilepton+Fake		Non-triggerable Dilepton + Triggerable Fake	
	#	Fake yield	fraction of fakes	Fake yield
e e e	4	0.081 ± 0.041	0.178	0.014 ± 0.007
e e μ	4	0.028 ± 0.014	0.159	0.004 ± 0.002
e μ μ	3	0.031 ± 0.018	0.219	0.007 ± 0.004
μ μ μ	10	0.150 ± 0.047	0.141	0.021 ± 0.007
Total background from fakes:				$\mathbf{0.34 \pm 0.07}$

Table 15: Trileptons in the Z mass region with $\not\!\!E_T > 25$ GeV.

Z+jets(s) to dominate, so this provides a check on our fake estimates. We also check the dilepton Z mass region dominated by the Drell-Yan process.

4.1 Dilepton Z Mass Region (Drell-Yan)

The Drell-Yan background by far a more important background for our $WW \rightarrow l\nu l\nu$ analysis where this background has been extensively studied. In [11], important checks of the Z cross section have been performed, where we measure $\sigma \times \text{BR}(\text{Z} \rightarrow \text{ee}) = 256.9 \pm 1.4\text{pb}^{-1}$ and $\sigma \times \text{BR}(\text{Z} \rightarrow \mu\mu) = 265.9 \pm 1.7\text{pb}^{-1}$, consistent with expectations. The WZ analysis shares, in large part, a common code base with the $WW \rightarrow l\nu l\nu$ analysis in terms of lepton reconstruction and ID, samples, etc., so the checks in CDF note 8096 are applicable here.

In this section, we show some of the kinematic distributions in the dilepton Z control region that have been generated in WZ analysis with relaxation of the third lepton requirement but still requiring opposite-sign same-flavor pairs in the Z mass region. Here we we use all of the same lepton categories we use in the trilepton analysis, including allowing the non-triggered leg to be $E_T > 10$ GeV.

Figures 6-9 show these distributions normalized to the expected number of events from Monte Carlo and reconstructed in data summed over both Gen5 and Gen 6 samples. We generally have good agreement in the shapes and normalizaton. We expect 34943 events and observe 36217 (+3.6%) for electrons. For muons, we expect 24191 events and observe 25336 events (+4.7%), which we consider acceptable given that the Run II measurement [12] of the Drell Yan cross section in Z$\rightarrow \mu\mu$ is measured to be 2.4% higher than the NLO prediction using the first 337pb^{-1}.

4.2 Trilepton Z Mass, Low $\not\!\!E_T$ Region

In this section, we show the trilepton data compared with our background expectations after full selection except the $\not\!\!E_T$ cut which is reversed to be < 20 GeV. Tables 16 and 17

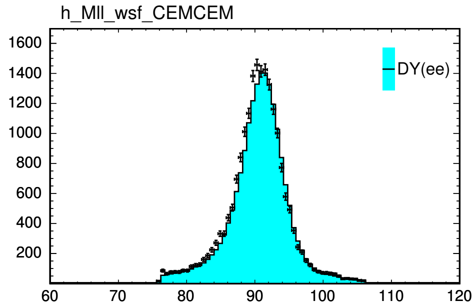

(a) Dilepton mass (GeV)

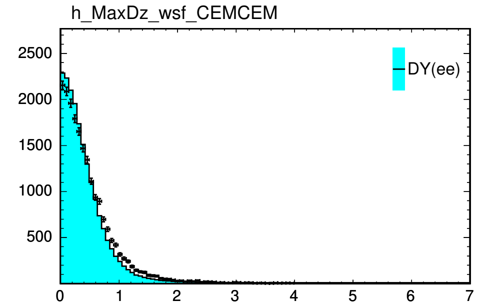

(b) Δz_0 between leptons (cm)

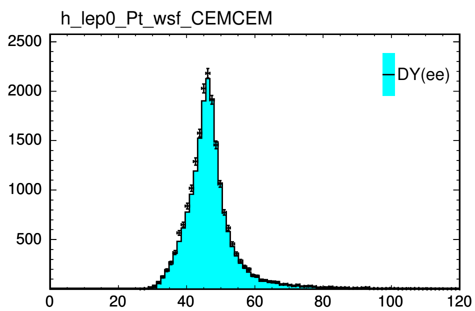

(c) Leading lepton p_t GeV

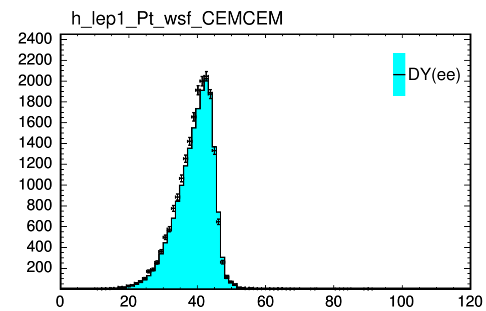

(d) Sub-leading lepton p_t GeV

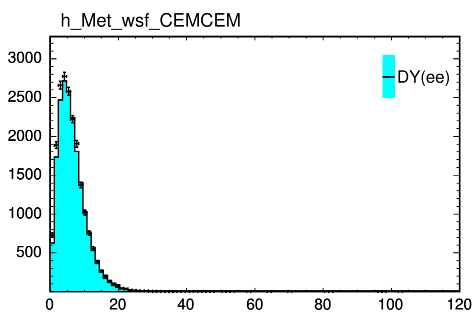

(e) $\not\!\!E_T$ GeV

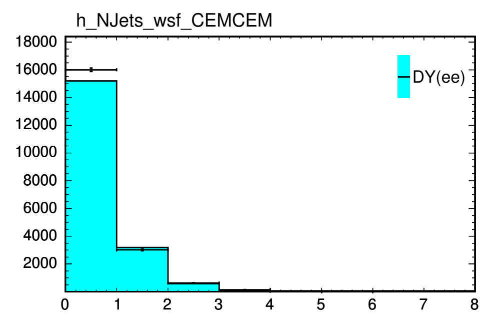

(f) Jet multiplicity

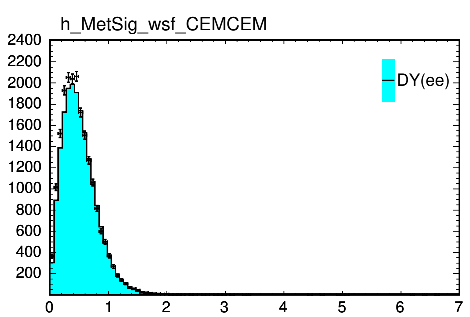

(g) $\not\!\!E_T$ significance

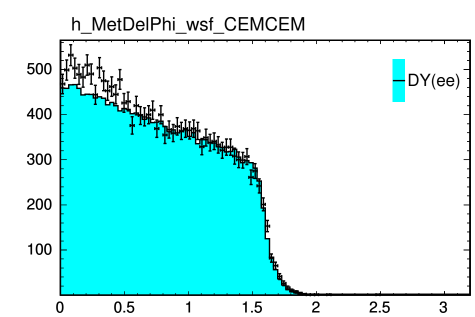

(h) $\Delta\phi(\not\!\!E_T$,nearest lepton,jet) (rad)

Figure 6: Kinematic distributions comparing data reconstructed as dileptons (CEM-CEM) and Drell-Yan Monte Carlo. Each normalized to events expected in full data set after selection cuts.

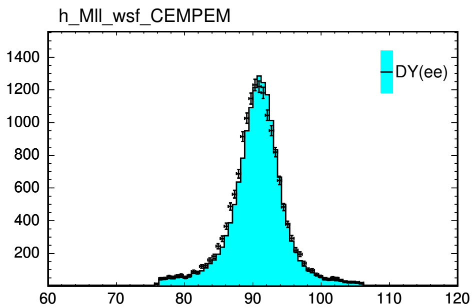

(a) Dilepton mass (GeV)

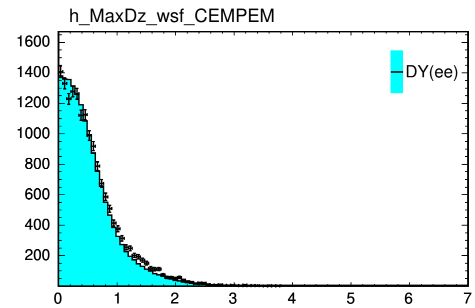

(b) Δz_0 between leptons (cm)

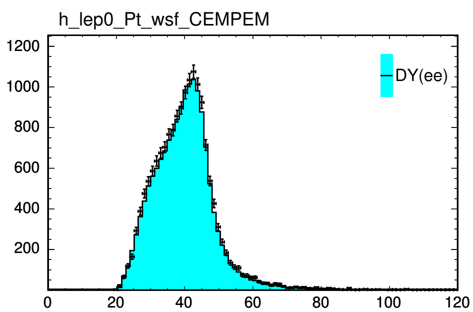

(c) Leading lepton p_t GeV

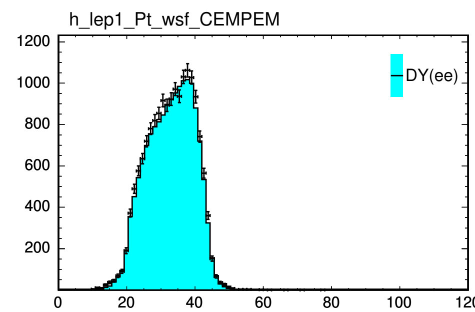

(d) Sub-leading lepton p_t GeV

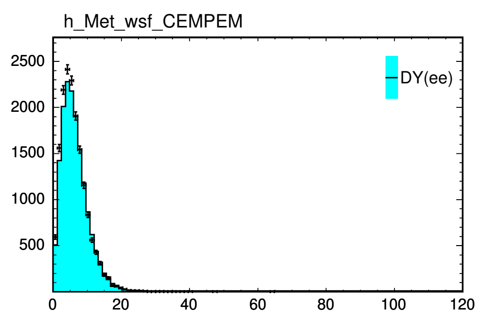

(e) $\not\!\!E_T$ GeV

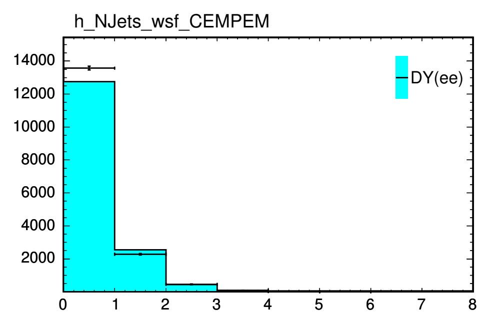

(f) Jet multiplicity

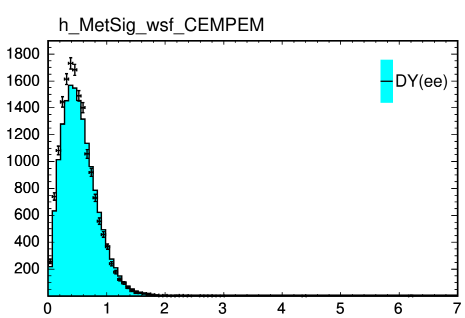

(g) $\not\!\!E_T$ significance

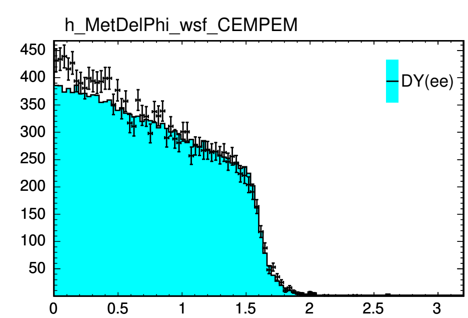

(h) $\Delta\phi(\not\!\!E_T$,nearest lepton,jet) (rad)

Figure 7: Kinematic distributions comparing data reconstructed as dileptons (CEM-PEM) and Drell-Yan Monte Carlo. Each normalized to events expected in full data set after selection cuts.

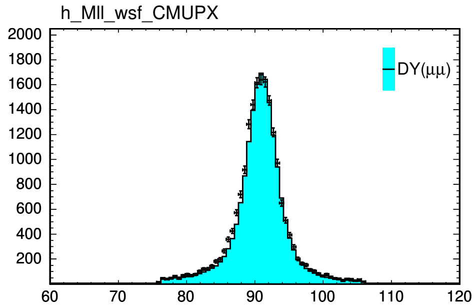

(a) Dilepton mass (GeV)

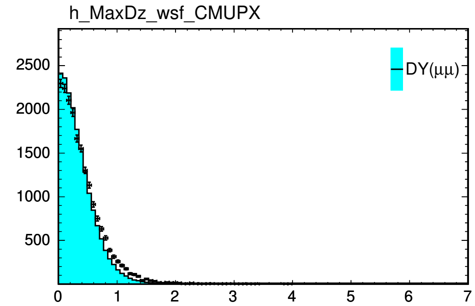

(b) Δz_0 between leptons (cm)

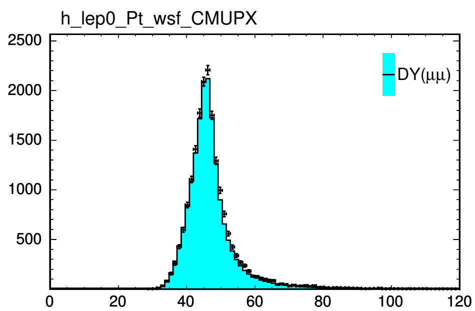

(c) Leading lepton p_t GeV

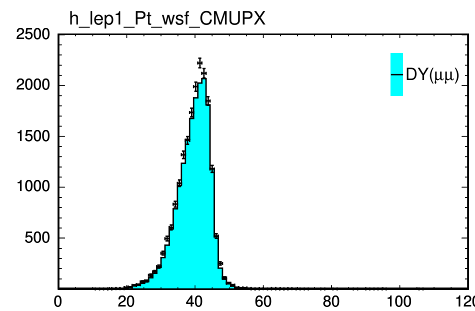

(d) Sub-leading lepton p_t GeV

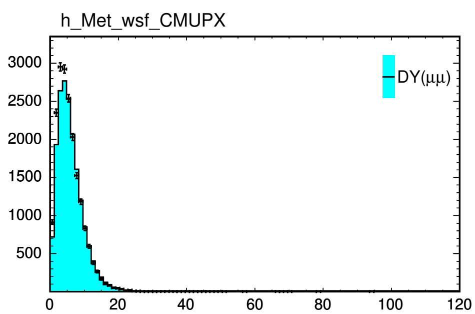

(e) $\not\!\!E_T$ GeV

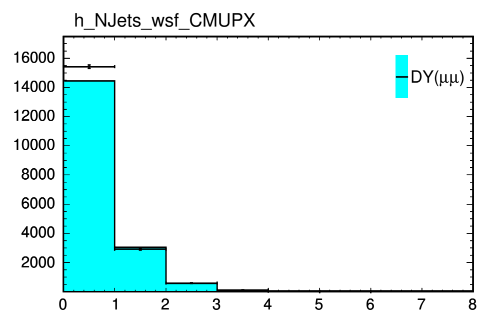

(f) Jet multiplicity

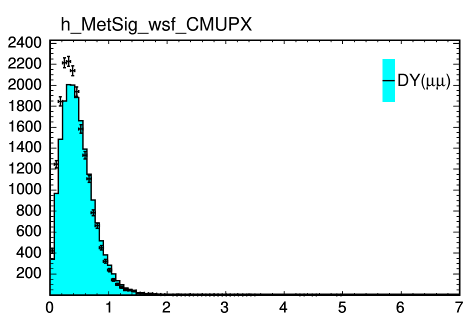

(g) $\not\!\!E_T$ significance

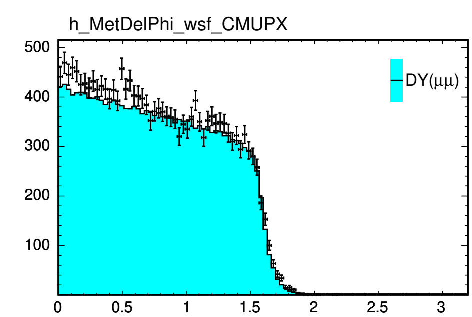

(h) $\Delta\phi(\not\!\!E_T$,nearest lepton,jet) (rad)

Figure 8: Kinematic distributions comparing data reconstructed as dileptons (CMUP-CMUP,CMX,CMIO) and Drell-Yan Monte Carlo. Each normalized to events expected in full data set after selection cuts.

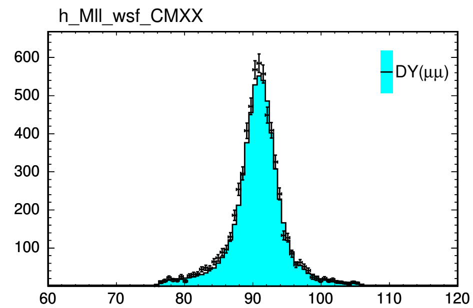

(a) Dilepton mass (GeV)

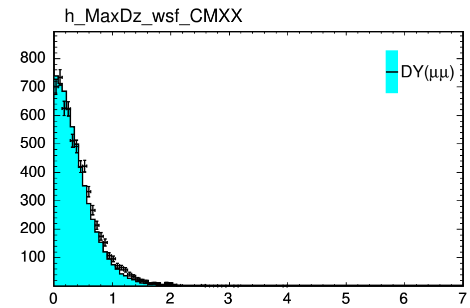

(b) Δz_0 between leptons (cm)

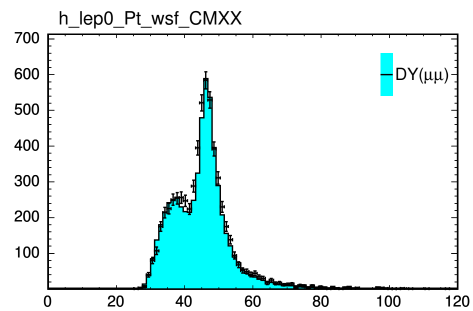

(c) Leading lepton p_t GeV

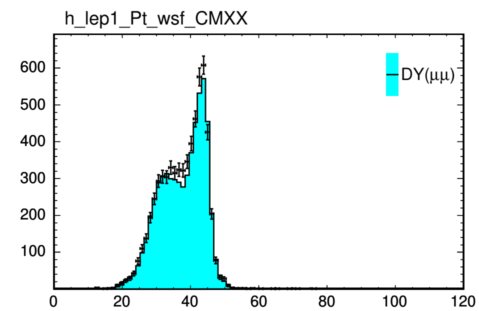

(d) Sub-leading lepton p_t GeV

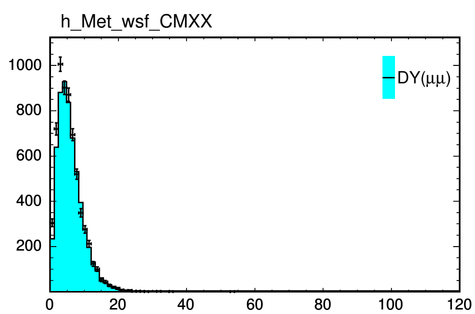

(e) $\not\!\!E_T$ GeV

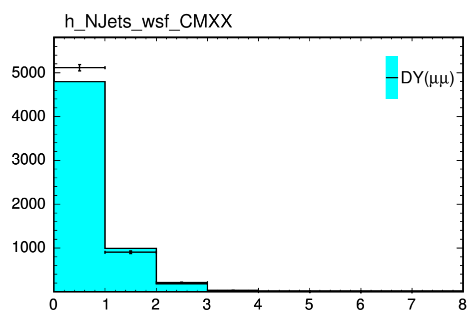

(f) Jet multiplicity

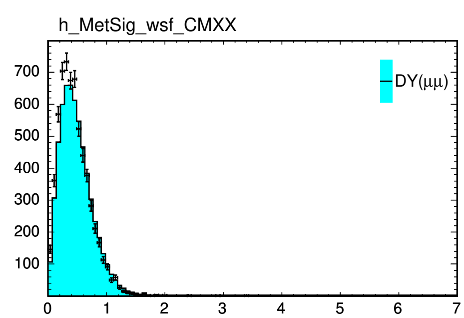

(g) $\not\!\!E_T$ significance

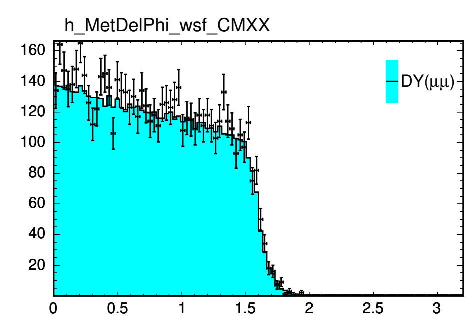

(h) $\Delta\phi(\not\!\!E_T$,nearest lepton,jet) (rad)

Figure 9: Kinematic distributions comparing data reconstructed as dileptons (CMX-CMUP,CMX,CMIO) and Drell-Yan Monte Carlo. Each normalized to events expected in full data set after selection cuts.

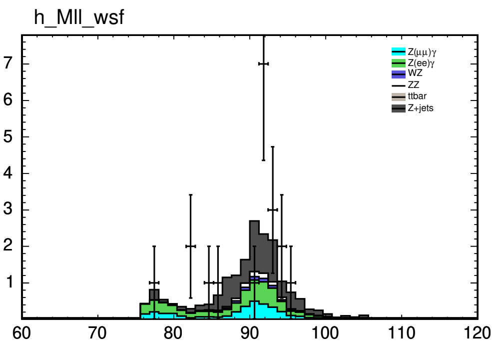

(a) Dilepton mass (GeV)

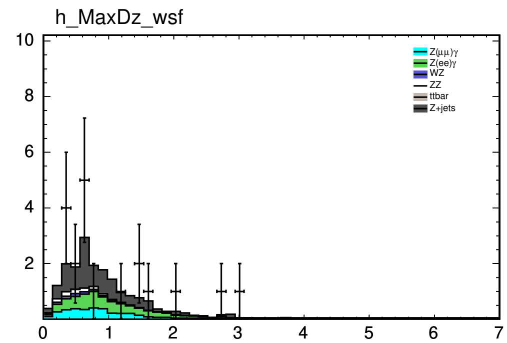

(b) Δz_0 between leptons (cm)

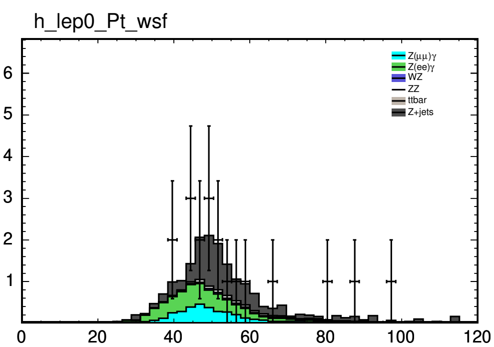

(c) Leading lepton p_t GeV

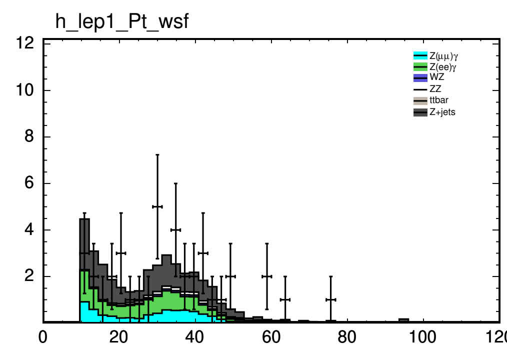

(d) Sub-leading lepton p_t GeV

Figure 10: Kinematic distributions comparing data reconstructed as trileptons in the low $\not\!\!E_T$ region with expected backgrounds from fakes and other physics backgrounds. Each normalized to events expected in full data set after selection cuts.

show that the total background expectation of 20.4±0.51 events is in good agreement with the 19 observed events in the trilepton, Z mass, low $\not\!\!E_T$ control region. In the breakdown by lepton category, it appears that there is only marginal agreement in the e$\mu\mu$ (6% probability to observe 3 or fewer events given 7.6 expected) and $\mu\mu\mu$ (7% probability to observe 3 or more events given 0.94 expected) categories. The eee and eeμ categories are in good agreement with expectations.

Figures 10 and 11 shows some distributions of event and background expectations normalized to the total number of expect events. The observed distributions are in agreement with expectations, within the (rather limited) statistics afforded by this control region.

category	$\not\!\!E_T < 20$ GeV
WZ	
e e e	0.168 ± 0.003
e e μ	0.142 ± 0.003
e μ μ	0.142 ± 0.003
μ μ μ	0.138 ± 0.003
Total	0.590 ± 0.006
ZZ	
e e e	0.337 ± 0.006
e e μ	0.123 ± 0.004
e μ μ	0.304 ± 0.006
μ μ μ	0.126 ± 0.004
Total	0.890 ± 0.010
$Z(e^+e^-)\gamma$	
e e e	5.206 ± 0.162
$Z(\mu^+\mu^-)\gamma$	
e μ μ	3.458 ± 0.133
Triggerable Dilepton+Fake	
e e e	4.35 ± 0.34
e e μ	0.71 ± 0.09
e μ μ	3.05 ± 0.29
μ μ μ	0.60 ± 0.08
Total	8.71 ± 0.46
Non-triggerable Dilepton+Triggerable Fake	
e e e	0.77 ± 0.06
e e μ	0.11 ± 0.01
e μ μ	0.67 ± 0.06
μ μ μ	0.08 ± 0.01
Total	1.63 ± 0.09

Table 16: Breakdown of expected contributions to trileptons in the Z mass control region with $\not\!\!E_T < 20$ GeV.

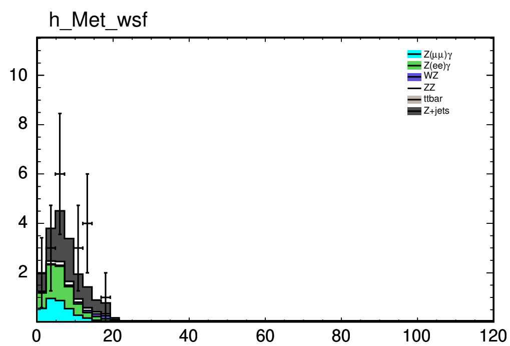

(a) $\not\!\!E_T$ GeV

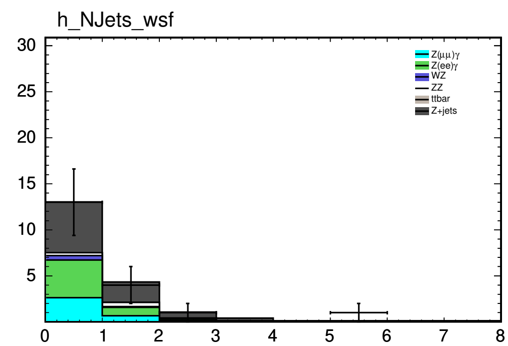

(b) Jet multiplicity

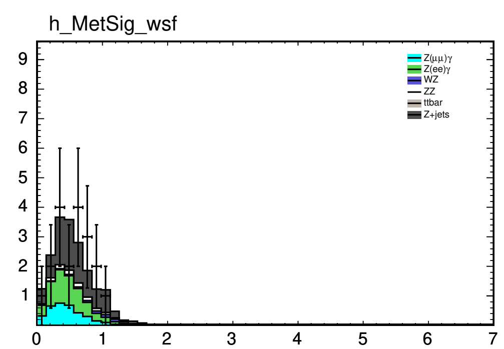

(c) $\not\!\!E_T$ significance

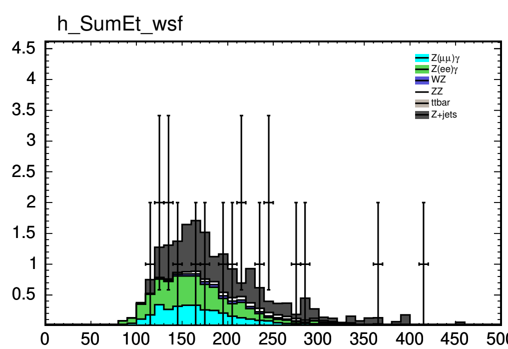

(d) $\sum E_t$

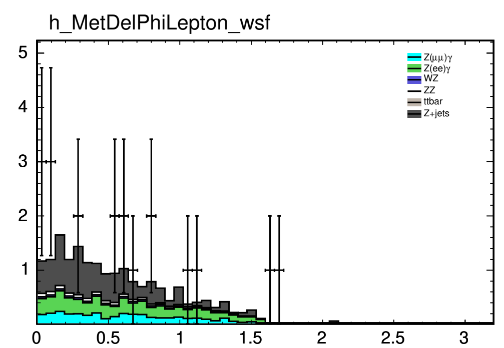

(e) $\Delta\phi(\not\!\!E_T$,nearest lepton) (rad)

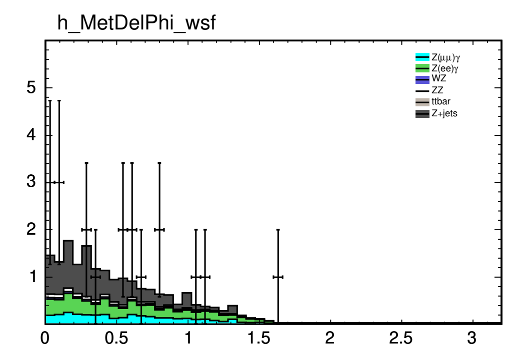

(f) $\Delta\phi(\not\!\!E_T$,nearest lepton or jet) (rad)

Figure 11: Kinematic distributions comparing data reconstructed as trileptons in the low $\not\!\!E_T$ region with expected backgrounds from fakes and other physics backgrounds. Each normalized to events expected in full data set after selection cuts.

category	Sum of backgrounds	Observed
e e e	10.8 ± 0.4	12
e e μ	1.1 ± 0.1	1
e μ μ	7.6 ± 0.3	3
μ μ μ	0.94 ± 0.08	3
Total	**20.5 ± 0.51**	**19**

Table 17: Expected and observed trileptons in the Z mass control region with $\not{E}_T <$ 20 GeV.

	run=199559, evt=6818215	run=202070, evt=407060
category	TCE LCE PHX	TCE TCE TCE
lepton$_0$ E_t (GeV)	(TCE) +69.8	(TCE) -93.0
lepton$_1$ E_t (GeV)	(LCE) -24.4	(TCE) -59.9
lepton$_2$ E_t (GeV)	(PHX) -22.5	(TCE) +38.6
$\not{E}_T$ (GeV)	27.6	38.5
$\sum E_t$ (GeV)	193.9	366.0
$\not{E}_T$ significance	1.98	2.01
$\Delta\phi(\not{E}_T$,lepton,jet) (deg)	20.8	0.65
N_{jets}	2	1
M_{01} (GeV)	101.6	179.8
M_{02} (GeV)	92.6	96.1
M_{12} (GeV)	86.7	109.1

Table 18: Trilepton candidates in the signal region

5 Candidates

We found two trilepton candidates passing our full selection. Figure 5 shows the $\not{E}_T$ distribution of our trilepton candidates, both in the Z region, low $\not{E}_T$ control region ($\not{E}_T$ < 20 GeV) and our signal region ($\not{E}_T$ > 25 GeV). Detailed information about the candidate events is summarized in Table 18. Event displays of both candidates are shown in Figures 5 and 5. Kinematic distributions comparing data the trilepton candidates in the signal region with expected WZ signal and backgrounds from fakes and other physics backgrounds are shown in Figures 16 and 17.

The Poisson probability for a mean background of 0.91 to fluctuate to 2 or more observed events is 23%. The probability of observing 2 or fewer events with an expectation of 4.63 events (total signal + background) is 16%. Therefore, we cannot claim we have observed WZ production in the trilepton channel and instead set limits on the production

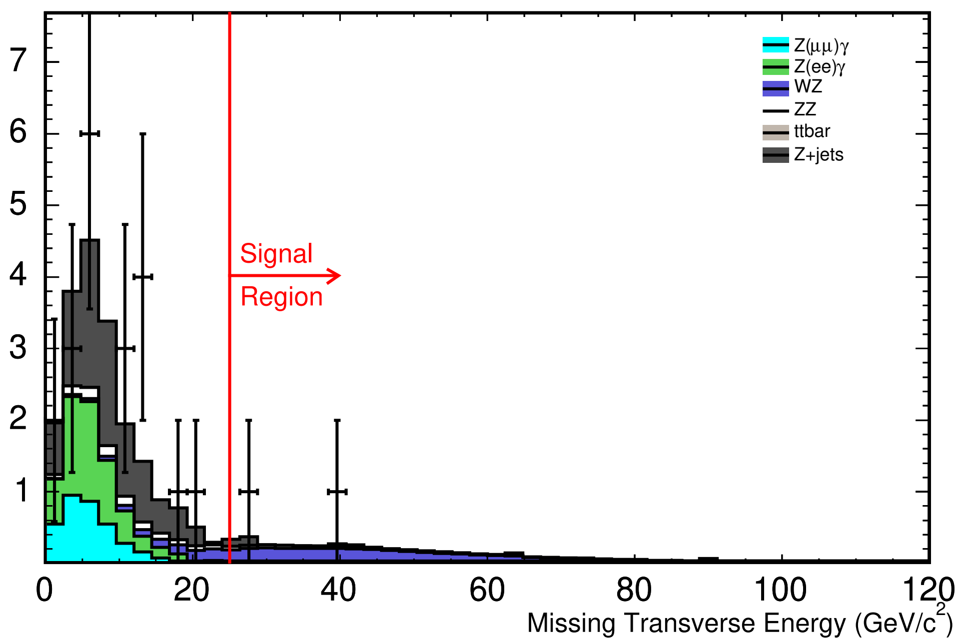

Figure 12: $\not\!\!E_T$ distribution of trilepton candidates.

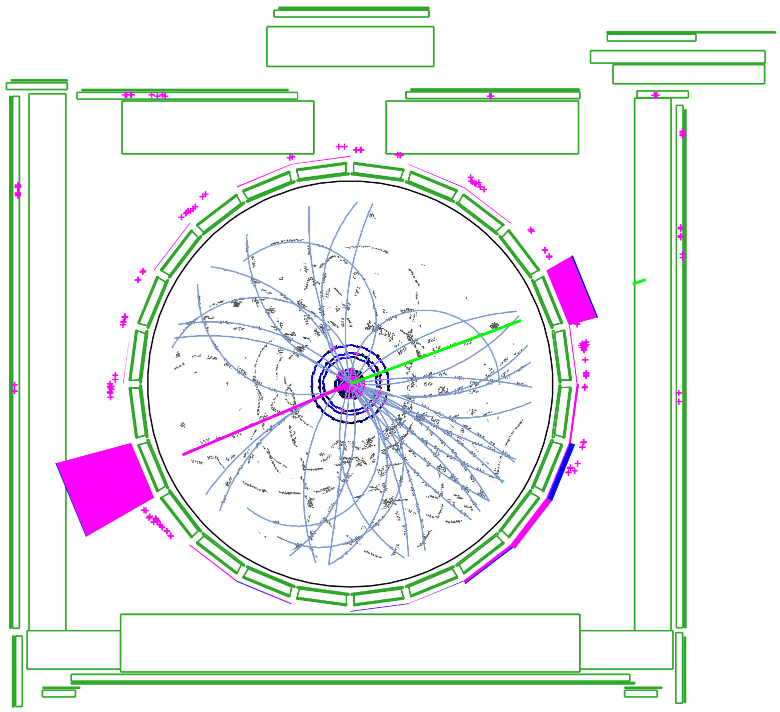

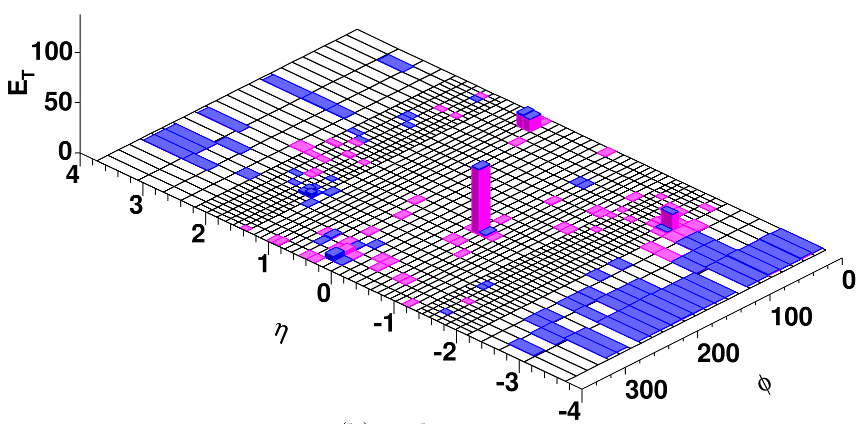

(b) Et lego view

Figure 13: Event display for trilepton candidate: run=199559, event=6818215

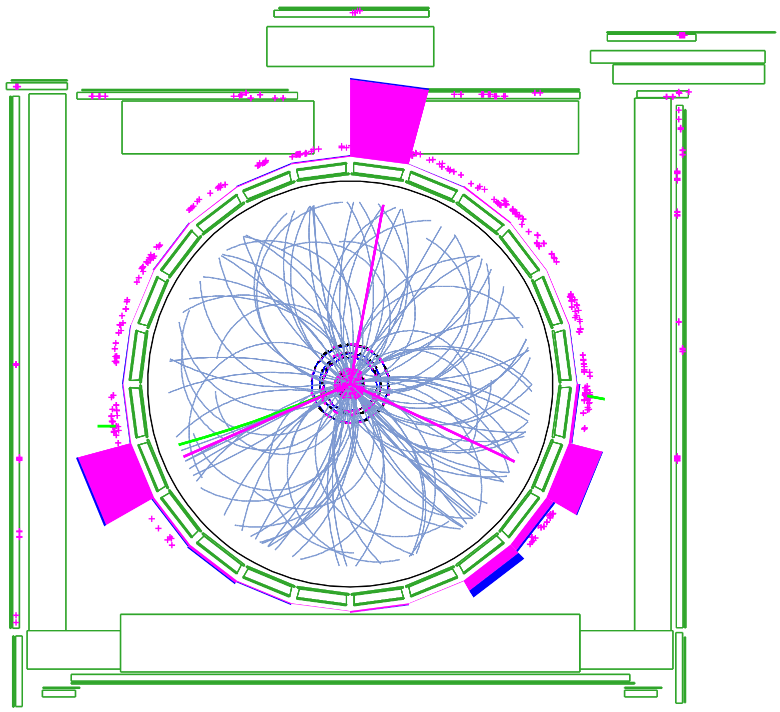

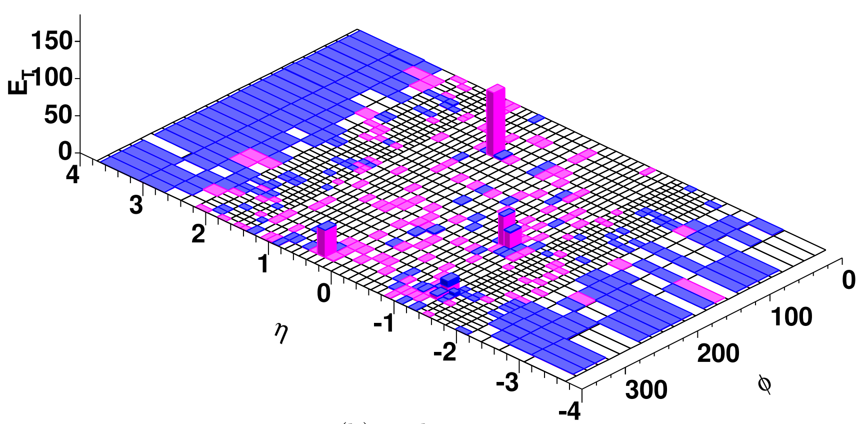

(b) Et lego view

Figure 14: Event display for trilepton candidate: run=202070, event=407060

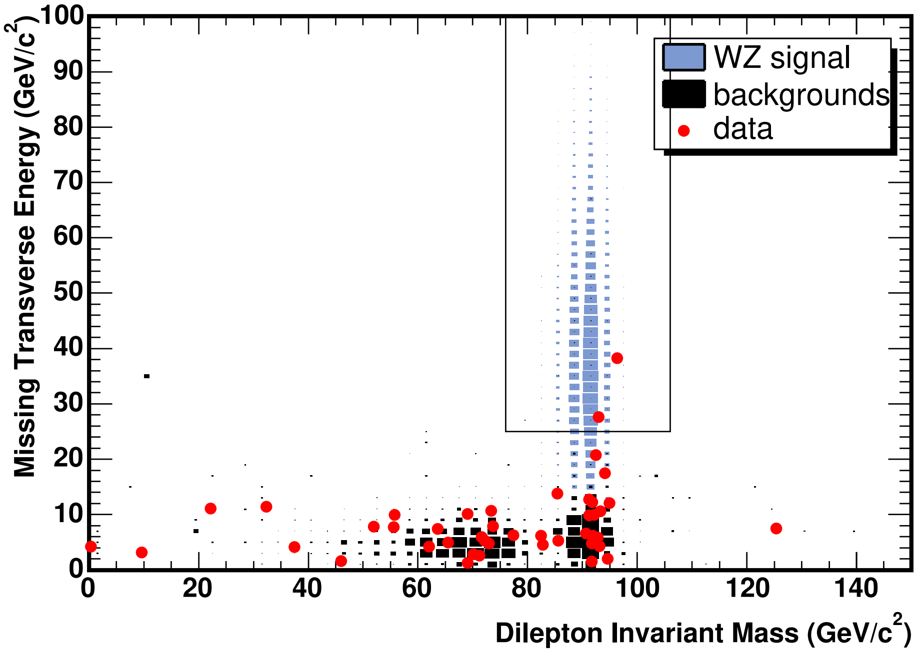

(a) Full mass range

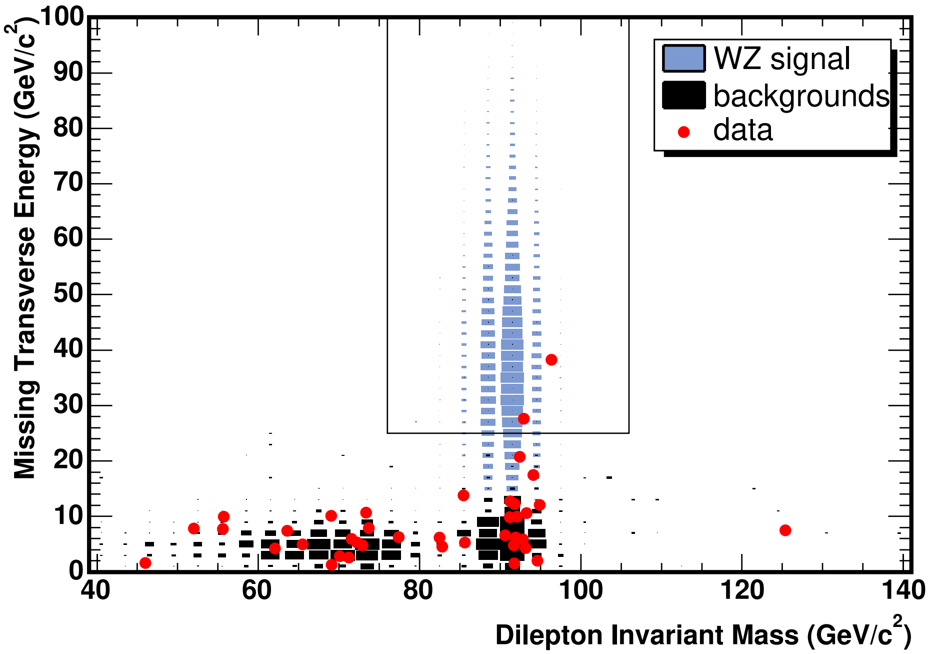

(b) Zoomed-in mass range

Figure 15: $\mathrm{M_{ll}}$ vs. $\not\!\!E_T$ for trilepton candidates.

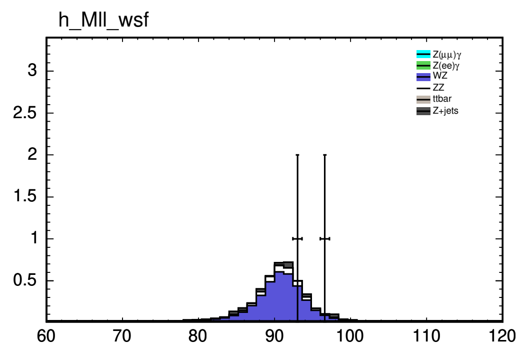

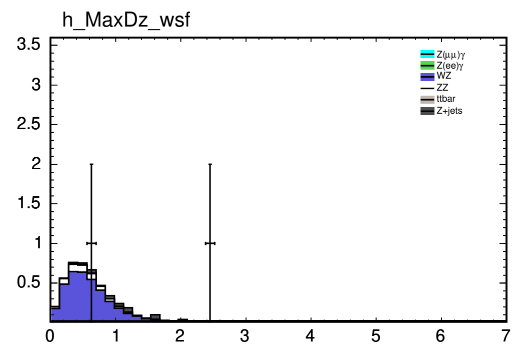

(a) Dilepton mass (GeV)

(b) Δz_0 between leptons (cm)

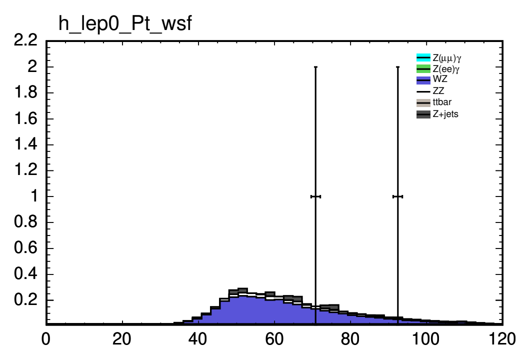

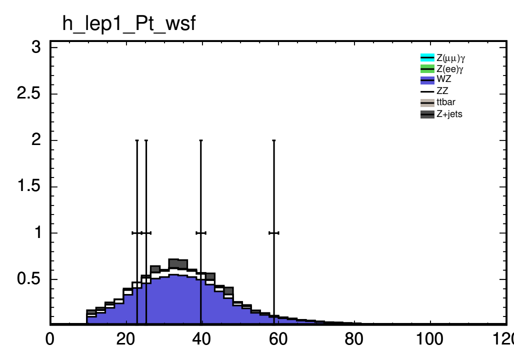

(c) Leading lepton p_t GeV

(d) Sub-leading lepton p_t GeV

Figure 16: Kinematic distributions comparing data reconstructed as trileptons in the signal region with expected backgrounds from fakes and other physics backgrounds. Each normalized to events expected in full data set after selection cuts.

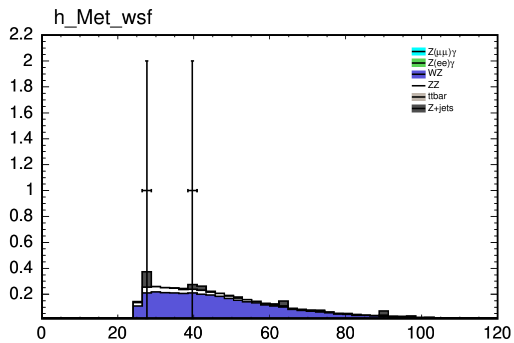

(a) $\not\!\!E_T$ GeV

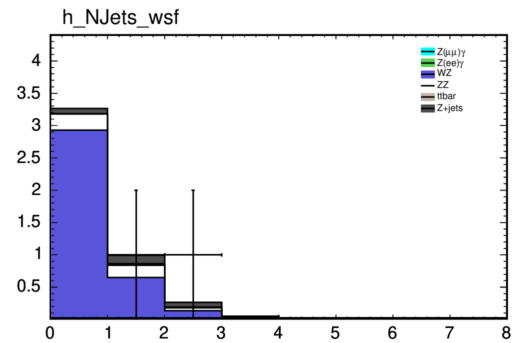

(b) Jet multiplicity

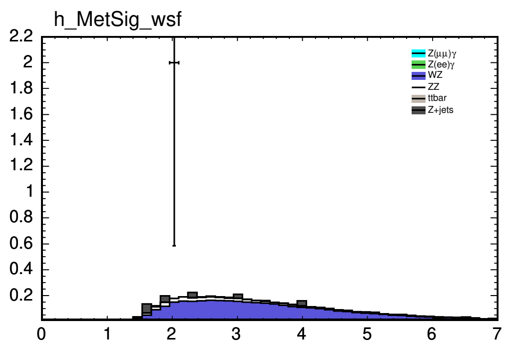

(c) $\not\!\!E_T$ significance

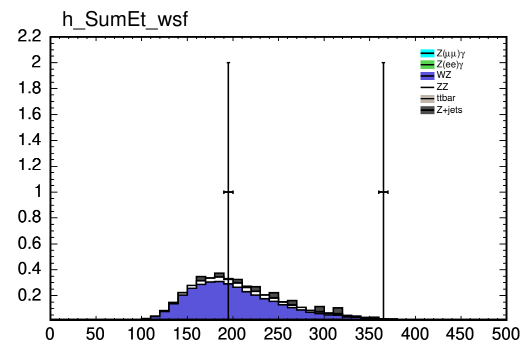

(d) $\sum E_t$

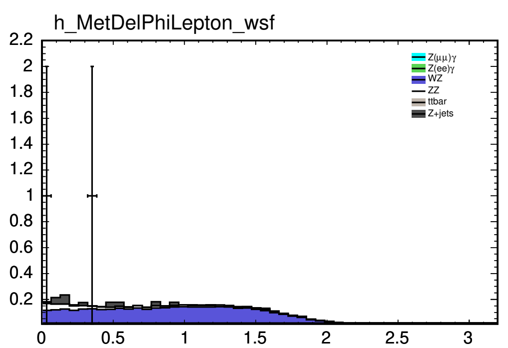

(e) $\Delta\phi(\not\!\!E_T$,nearest lepton) (rad)

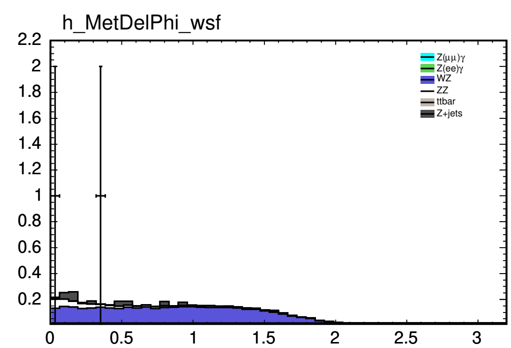

(f) $\Delta\phi(\not\!\!E_T$,nearest lepton or jet) (rad)

Figure 17: Kinematic distributions comparing data reconstructed as trileptons in the signal region with expected backgrounds from fakes and other physics backgrounds. Each normalized to events expected in full data set after selection cuts.

cross section.

6 Systematics

In this section we assess the systematics on our WZ cross section determination.

6.1 Signal and Background acceptance

6.1.1 Jet Energy Scale

Since we do not make an explicit cut on jet multiplicity but rather jets are used only to correct the $\not{E}_T$, we do not assign a systematic due to jet energy scale.

6.1.2 Lepton ID Scale Factors

The lepton ID scale factor uncertainties have been propagated through the analysis. Significant contribution to the systematic uncertainty is due to the low pt scale factors. The observed shifts in expected signal and background yields are: 2% for WZ, 3% for ZZ, 4% for $Z\gamma$ and 2% for $t\bar{t}$ which we include as our systematic uncertainty on acceptance.

6.1.3 Trigger efficiency

The statistical uncertainties on the trigger efficiency measurements are small and found to contribute less than 1% to the acceptance uncertainty. We also consider the variation in acceptance if we allow our loose CEM category to contribute to the trigger and also the effect of the trigger turn-on curve(s) (recall that we allow sub-leading lepton legs to have $10 < \text{Pt} < 20$ GeV. Including the loose CEM leg as triggerable legs increased the WZ acceptance by 0.2% and the ZZ acceptance by 0.4%. The effect on the other backgrounds was negligible. Rather than use the detailed trigger efficiency curves, we lower the Pt requirement for a triggerable leg from 20 GeV to 16 GeV, where we would expect the trigger efficiency (CEM) to be 10% according to [13]. This increased the WZ acceptance by 1.7% and the ZZ acceptance by 2.0%, with changes to the other backgrounds being negligible. Considering these effects, we conservatively assign a systematic uncertainty of 2.0% for the WZ and ZZ acceptance due to trigger efficiency.

6.1.4 PDF Systematics

The sensitivity of the acceptance to the choice PDF has been studied for WW in [11] and also WZ, ZZ in [6]. In both cases, they arrive at 2% systemtic uncertainty on the acceptance due to PDF shape, which is the uncertainty we quote for WZ.

6.1.5 Energy Scale/Resolution

In Figures 6(a), 6(a), 6(a), and 6(a) we showed the comparison between data and Monte Carlo for the dilepton invariant mass distributions. We have applied the Joint Physics recommended energy scaling to the Monte Carlo so these are in good agreement. Gaussian fits to the core of these distributions yields scale differences with are 0.3% for ee and 0.1% for $\mu\mu$ and resolution differences which are 2.8% for CEM-CEM, 5.3% for CEM-PEM, and 3.5% for $\mu\mu$. Given our loose cut on invariant mass of (76, 106) GeV, the systematic from energy scale and resolution is determined from appropriate shifting and smearing of the Monte Carlo distribution to be very small, for which we assign a conservative 1% uncertainty on the signal and background acceptances for Z+X.

6.1.6 $\not{E}_T$ Modeling

The $\not{E}_T$ modeling systematic uncertainty the WW signal acceptance was determined in CDF 8094[11] using a re-weighting technique to be very small: 0.3%. Although the $\not{E}_T$ distributions are slightly different for WW, WZ, and ZZ, the $\not{E}_T$ calculation for both analysis is identical and so we assign a conservative systematic uncertainty of 1.0% for both WZ and ZZ.

6.1.7 Fake Background

We have propagated the systematic uncertainties on the fake backgrounds (shown by the solid band in Figures 4 and 5, which arises from the difference between the different jet samples. This is found to be $^{45\%}_{26\%}$ on our determination of the fake background. The asymmetric error is due to the currently not understood discrepency between the Monte Carlo and jet data fake rates for PHX, as described detail in CDF 8093[10].

6.1.8 Conversion Scale Factor for Zγ

The Zγ mode enters our selection when the photon is reconstructed as an electron and we also have large $\not{E}_T$. This is usually due to a conversion. In the TCE selection, we explicitly veto conversions, but the efficiency of this veto may not be well modeled in the Monte Carlo.

Based upon the studies in CDF Note 8073[9] Attal et al. on the conversion modeling, and ombining the conversion scale factor, material uncertainty, and normalization uncertainty, we apply a 20% systematic uncertainty on the Zγ background. This uncertainty dominates other uncertanties such a k-factor uncertainties for the difference between LO and NLO cross-sections.

Source	Uncertainty
Jet Multiplicity	-
Lepton ID	2%
Trigger Efficiency	2%
$\not\!\!E_T$ Modeling	1%
Energy Scale/Resolution	1%
PDF	2%
Total	4%

Table 19: Systematics on WZ Acceptance

6.1.9 ZZ Cross Section

For the ZZ cross-section uncertainty, we take the half the difference between LO and NLO cross section as an estimate of the effect of higher or calculation. This is 10% ZZ cross section, which we assign as a systematic uncertainty.

6.2 Summary

A summary of the WZ acceptance systematic uncertainties is shown in Table 19. The total systematic uncertainty on the WZ acceptance is 3%. Our total expected yield for WZ in trileptons, not including the cross section or luminosity errors, is

$$3.72 \pm 0.02(\text{stat.}) \pm 0.15(\text{syst.})$$

The expected background yields are:

- Zγ: 0.025 $\pm$ 0.011 (stat.) $\pm$ 0.005 (syst.)
- ZZ: 0.498 $\pm$ 0.007 (stat.) $\pm$ 0.055 (syst.)
- ttbar: 0.047 $\pm$ 0.010 (stat) $\pm$ 0.005 (syst.)
- Z+jets (fakes): 0.34 $\pm$ 0.07 (stat.) $^{+0.15}_{-0.09}$ (syst.)

The total background expectation is

$$0.91 \pm 0.07(stat.)^{+0.16}_{-0.10}(syst.)$$

7 Cross Section

The cross-section limit is calculated using a modified version of the technique suggested by Feldman and Cousins [14]. Their technique as does not allow for the uncertainty on the background estimate to be directly propagated into the confidence interval calculation. We have written a toy Monte Carlo based implementation of the Feldman-Cousin interval calculation that returns the same intervals as their paper for zero background uncertainty, but allows us to include the systematic uncertainty on the background estimate, acceptance and luminosity. The final results is $\sigma(WZ) < 6.335\ pb$ at the 95% confidence level.

7.1 Details of the limit calculator

The interval is calculated in two steps. Reading the Feldman and Cousins paper will help with the following explanation.

For each possible value of the cross-section, an acceptance interval is calculated. This is the range of possible observations which include 95% of the probability. There is choice for this interval (any set including 95% is statistically valid). We follow the Feldman-Cousins ranking procedure. The acceptance interval is determined by toy Monte Carlo. We generate a set of possion experiments in which the prediction is varied based on the systematic uncertainties. The prediction inputs are the luminosity-dependent background, $B_{\mathrm{lumi-dep}}$, the luminosity-independent background, $B_{\mathrm{lumi-indep}}$, the acceptance, A, and the luminosity, $\mathcal{L}$. The calculation is then

$$N_{\mathrm{expected}} = \tilde{A}\tilde{\mathcal{L}}\sigma + \frac{\tilde{\mathcal{L}}}{\mathcal{L}}\tilde{B}_{\mathrm{lumi-dep}} + \tilde{B}_{\mathrm{lumi-indep}}, \tag{3}$$

where $\tilde{}$ denotes the varied version of the variable and σ is the cross-section for which the acceptance interval is being calculated. The range including the top 95% of the ranked experiments is the acceptance interval.

The confidence interval is then the range possible values of the cross-section for which the acceptance interval includes the number of observed events.

We have preformed two cross-checks of implementation. First the systematic uncertainties were set to zero and the results were compared with the **TFeldmanCousins** ROOT class. The second check with the full systematics is that 95% of experiments produce intervals which contain the generate cross-section.

8 Summary and Conclusions

We have searched for WZ production is trileptons + $\not\!\!E_T$ using $824.5\ pb^{-1}$ of integrated luminosity. We expect 3.72±0.02(stat.)±0.15(syst.) events of signal and $0.91\pm0.07(stat.)^{+0.16}_{-0.10}(syst.)$ events of background. We observed two trilepton candidates passing our selection, consistent both with a fluctuation of the background alone as well as the background + signal expectation. Using these results, we set a limit on the WZ cross section at $\sqrt{s} = 1.96$ TeV of 6.35 pb at 95% confidence.

References

[1] The D0 Collaboration, Phys. Rev. **D71**, 091105 (2005)

[2] The CDF Collaboration, Phys. Rev. Lett. 95 141802 (2005)

[3] J.M.Campbell and R.K.Ellis, Phys. Rev. **D60**, 113006 (1999)

[4] W.Giele *et al.*, hep-ph/0204316

[5] BaurMC reference

[6] S. Cabrera, J. Deng, A. Goshaw, C. Hays, Y. Huang, M. Kruse, "Measurement of the ZZ + ZW Cross section using Run II Data" CDF Note 6920.

[7] Veronique Boisvert, "Trigger Efficiencies for the High ET Central Electrons in Gen6", CDF Note 7939

[8] U. Grundler, A. Taffard, X. Zhang, "High-Pt muons recommended cuts & efficiencies for Winter 2006", CDF Note 7956

[9] Alon Attal, Anadi Canepa, "Photon Conversion Removal Efficiency", CDF Note 8037

[10] Shih-Chieh Hsu, Elliot Lipeles, Kevin McCarthy, Mark Neubauer, Frank Würthwein, "Lepton ID and Fake Rates for the WW and WZ Analyses", CDF Note 8093

[11] Shih-Chieh Hsu, Elliot Lipeles, Kevin McCarthy, Mark Neubauer, Frank Würthwein, "Measurement of the WW Cross Section using 0.8fb^{-1}", CDF Note 8094

[12] W. David Dagenhart, "Measurement of the Z Production Cross Section", CDF Note 7865

[13] Young-Kee Kim, *et al*, "Trigger Efficiencies for High P_T Electrons", CDF Note 6234

[14] Gary J. Feldman and Robert D. Cousins, "A Unified Approach to the Classical Statistical Analysis of Small Signals", Phys. Rev. **D57**, (1998) 3873-3889